The Sharamurunian rodent fauna in the Erlian Basin, Nei Mongol, China

LI Qi[1,2] LI Qian[2,3*]

(1 *Centre for Vertebrate Evolutionary Biology*, *Yunnan University* Kunming 650500)
(2 *Key Laboratory of Vertebrate Evolution and Human Origins of Chinese Academy of Sciences*, *Institute of Vertebrate Paleontology and Paleoanthropology*, *Chinese Academy of Sciences* Beijing 100044)
(3 *CAS center for Excellence in Life and Paleoenviroment* Beijing 100044)
* Corresponding author: liqian@ivpp.ac.cn

Abstract New middle Eocene rodent fossils discovered from the lower part of the Shara Murun Formation of Ula Usu, Erlian Basin, Nei Mongol, China, the classical locality of Sharamurunian mammalian fauna, were identified as 9 separate species (the ctenodactyloids *Yuomys cavioides*, *Gobiomys neimongolensis*, *G. exiguus*, and *G. asiaticus*, the dipodids *Allosminthus uniconjugatus* and *Primisminthus shanghenus*, the cricetid *Pappocricetodon rencunensis*, the ischyromyid *Hulgana* cf. *H. ertnia*, and the cylindrodontid *Proardynomys ulausuensis*) belonging to 7 genera, 4 families, and 1 superfamily of Rodentia. The Ula Usu rodent assemblage shares a high degree of similarity with that from the "Lower Red" beds of the Erden Obo, and they both represent the typical Sharamurunian rodent assemblages found in northern China. The Sharamurunian rodent fauna in the Erlian Basin is analyzed by the minimum number of individuals based on the rodent materials from the lower part of the Shara Murun Formation in the Ula Usu and the "Lower Red" beds of the Erden Obo. In the Sharamurunian rodent fauna of the Erlian Basin, ctenodactyloids are the most dominant elements, and dipodids and cricetids follow next in prevalence. By analyzing the evolution of the rodent species richness in the Erlian Basin, the rodent faunas show a transformation from a ctenodactyloid dominant assemblage to a cricetid-dipodid dominant one in chronological order. The Sharamurunian rodent fauna from the Erlian Basin differs from that of the Yuanqu Basin and the differences in the rodent assemblages may be a response to the differences between the regional environments.

Key words Nei Mongol, Erlian Basin, Ula Usu, Sharamurunian, rodent fauna

Citation Li Q, Li Q, in press. The Sharamurunian rodent fauna in the Erlian Basin, Nei Mongol, China. Vertebrata PalAsiatica.

1 Introduction

Following the principle of North American Land Mammal Ages (NALMA), Romer (1966) proposed some related Asian Paleogene Land Mammal Ages (APLMA) on the basis

国家自然科学基金(批准号：42072023)、中国科学院战略性先导科技专项（编号：XDB26000000, XDA20070203)和中国科学院古生物化石发掘与修理专项资助。
投稿日期：2022-09-15

of mammalian faunas from different stratigraphic levels. Most of the APLMA proposed by Romer were derived from the selected Paleogene mammal faunas found in the Erlian Basin, Nei Mongol, such as Arshantan, Irdinmanhan, and Sharamurunian. After Romer, different researchers renamed the related land mammal and re-estimated their age (Li and Ting, 1983; Woodburne et al., 1987; Tong et al., 1995; Wang, 1997a, b).

The named locality of the Sharamurunian fauna is Ula Usu in the Erlian Basin, Nei Mongol. In the Sharamurunian mammalian fauna, perissodactyls were the most predominant. Then, artiodactyls became more diversified, and the ruminants appeared (Wang et al., 2007). However, studies on the Sharamurunian rodent fossils were very limited at Ula Usu, which is the classical locality of the Sharamurunian mammal fauna. Only Li (1975) reported on a few materials of *Yuomys*. Through the efforts of several years of field expeditions (2009–2017), a large number of rodent fossils were found at Ula Usu. This study focuses on the systematics of these new rodent materials, which complemented the Sharamurunian mammalian fauna in the Erlian Basin and improved the successional sequence of rodent assemblages through the early Eocene to early Oligocene in the Erlian Basin.

2 Geological setting

Ula Usu proper is the type locality for both the Shara Murun Formation and the Tukhum Formation. The upper part of the Shara Murun Formation consists of white and light gray sandstone, whereas the lower part consists of variegated sandy clay (Berkey and Morris, 1927; Chow and Rozhdestevensky, 1960; Bai et al., 2018). Below the Shara Murun Formation lies an interval of hard red clay (Granger, 1925), which Berkey and Morris (1927) named the Tukhum Formation. In recent field investigations, we remeasured the lithological strata in this area.

Eight distinct sedimentary layers are exposed at Ula Usu (Fig. 1). The lowermost layer (layer 1, 0–13.50 m) is the Tukhum Formation, which consists of muddy dark red siltstone and silty mudstone and has yielded a few perissodactyl fossils. Layer 2 (13.50–28.50 m), the bed from which the new rodent fossils reported on here come, is dominated by grayish green and dark red mudstone or silty mudstone. Layer 3 (28.50–45.00 m) is composed of grayish green mudstone and has yielded abundant postcranial bones and cheek teeth from perissodactyls and artiodactyls. Layer 4 (45.00–49.00 m) is made of grayish white silty mudstone and fine sandstone in the upper part and has yielded many perissodactyl fossils. Layer 5 (49.00–55.15 m) is a composed of white fine sandstone and siltstone interspersed with grayish green pebbled silty mudstone, which is rich in large calcareous nodules. Layer 6 (55.15–57.40 m) is dominated by light red mudstone with some Fe-Mn nodules. Layer 7 (57.40–59.27 m) is white gravelly coarse sandstone or fine sandstone. Layer 8 is the Quaternary cover.

All newly described specimens were collected from Layer 2 in the section, which is the lower part of the Shara Murun Formation at Ula Usu to which several field expeditions were carried out between 2009–2017 by a team from the IVPP (Fig. 1).

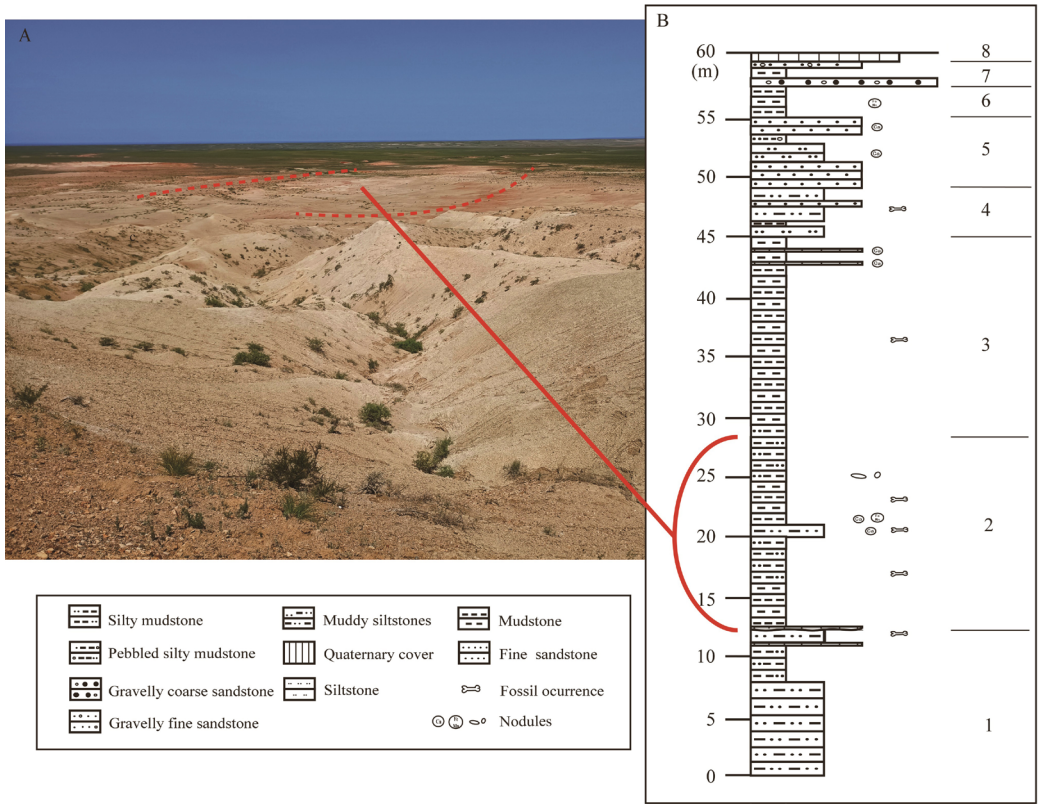

Fig. 1 Stratigraphy section of Ula Usu

A. the Paleogene outcrop at Ula Usu; B. stratigraphic section of the studied sediment series at Ula Usu The area circled by the red dotted line in the A-graph is the strata where new rodent fossils were collected, which was produced in between 30 m and 10 m of the stratigraphic column in the B-graph

3 Material and methods

Dental terminology generally follows Wang (1997a, 2019b) and Li and Meng (2015) for ctenodactyloids, Li (2018) and Wang et al. (2020) for cricetids and dipodids, Dashzeveg and Meng (1998) for ischyromyids, and Wang (2019a) for cylindrodontids. The measurements of the teeth were taken using a reticle with an accuracy of 0.01 mm mounted in a LEICA S9D microscope. The specimens were CT-scanned using a GE v|tome|x m 300&180 micro-computed-tomography scanner (GE Measurement & Control Solutions, Wuntsdorf, Germany) housed at the Key Laboratory of Vertebrate Evolution and Human Origins of Chinese Academy of Sciences. The graphic processing was done using the VGstudio Max 2.1 software (Volume Graphics, Genuine authorized). The analysis of rodent assemblages used the minimum number of individuals (MNI) that refers to the fewest possible number of people or animals in a skeletal assemblage. The MNI for each group was calculated from the total specimens by first separating the elements (teeth or bones) into left and right, and then counting the total of each element and selecting the maximum among them (Rose, 1981; Tong, 1997). All fossil

specimens collected are housed at the IVPP and are available for examination by qualified researchers.

Abbreviation IVPP, the Institute of Vertebrate Paleontology and Paleoanthropology, Chinese Academy of Sciences. AMNH, American Museum of Natural History, New York. PSS, Paleontology and Stratigraphy Section of Geological Institute, Mongolian Academy of Sciences. The measurement value "—" represents a partially broken specimen with no measurement data.

4 Systematics

Rodentia Bowdich, 1821

Cylindrodontidae Miller & Gidley, 1918

***Proardynomys* Dashzeveg & Meng, 1998**

***Proardynomys ulausuensis* sp. nov.**

Holotype IVPP V28608, a right mandible with p4–m3.

Locality and horizon Ula Usu, Erlian Basin, Nei Mongol; the lower part of the Shara Murun Formation.

Diagnosis Smallest species of the genus. Its lower cheek teeth have a narrow sinusid and short posterolophid. It differs from *P. borkhoii* in having a narrower sinusid and a shorter posterolophid on the lower cheek teeth, as well as a straighter ectolophid and more developed lophids on the m3. It differs from *Proardynomys* sp. in having a stronger posterolophid and a more buccally positioned ectolophid on the lower cheek teeth.

Etymology The specific epithet is derived from the type locality Ula Usu.

Measurements see Table 1.

Description The right mandible (IVPP V28608) is broken. The horizontal ramus is straight and strong, and the highest point of the horizontal ramus of the mandible is 0.95 cm, which is measured at the m2. The masseteric fossa anteriorly extends to between the m1 and m2 (Fig. 2). A small mental foramen is located below the trigonid of the m1.

The lower cheek teeth are low crowns, and have four transverse lophs. On the p4, the protoconid and the metaconid are well developed, and the protoconid is larger and lower than the metaconid after wear. The metalophid I is absent and the trigonid basin opens forward. The metalophid II is low, connecting the protoconid and the metaconid. Compared to the metaconid and entoconid, the hypoconid is larger and anterolabially extends clearly beyond the labial margin of the protoconid. The anterolabially elongation of the hypoconid gradually decreases from the p4 to m3. The metastylid crest extends backwards from the metaconid along the lingual edge of the crown and is separated from the entoconid by only a narrow groove. The ectolophid extends from the posterolabial of the protoconid to the anterolingual of the hypoconid. There is no mesoconid on the ectolophid. The hypolophid is thin and connects the entoconid to the hypoconid. The posterosinusid between the hypolophid and posterolophid is narrow and opens lingually. The sinusid is deep, wide, and opens anterolabially (Fig. 2).

On the m1, the talonid is wider than the trigonid, and the protoconid is lower than the metaconid. The straight metalophid I connects the protoconid and the metaconid and forms the anterior edge of the tooth. The metalophid II extends anterolingually to the metaconid and encloses the trigonid posteriorly. After wear, the hypoconid is similar to the protoconid in size. The metastylid crest is well developed, and a well-developed mesostylid is present on the metastylid crest (Fig. 2). The ectolophid is short but strong, and the mesoconid is missing on the ectolophid. The hypolophid is complete and straight, dividing the talonid basin into a broad mesosinusid and a narrow posterosinusid. The sinusid opens anterolabially and is narrower than that on the p4. The ectostylid in the sinusid is well developed. The posterolophid is strong but the hypoconulid is less developed.

The morphology of the m2 is similar to that of the m1, but the m2 is larger in size (Table 1). The trigonid of the m2 is slightly narrower than the talonid, but the width of the trigonid is slightly wider than that of the talonid on the m1. The protoconid is higher than the metaconid. The deep sinusid is wider than that of the m1. The ectostylid on the m2 is less developed than that on the m1.

The m3 is slightly longer than the m1 and m2. The trigonid of the m3 is relatively wider but longer than those of the m1 and m2. The mesostylid and metastylid crest are distinct. There is no mesoconid, ectostylid, and mesolophid (Fig. 2).

Comparisons The new material shares the following features with cylindrodontids: four transverse lophids, a well-developed mesostylid, and absence of mesolophid on p4–m3, weak hypolophid close to the posterolophid on the p4, complete ectolophid and hypolophid, and the metalophid directed toward the buccal side of the metaconid on m1–3. It differs from *Cylindrodon* (Douglass, 1901) in having the larger lower cheek teeth, the p4 is longer than the m1, and there is a thin hypolophid on the p4. *Pseudocylindrondon* (Burke, 1935) differs from the new material in having a smaller size, two mental foramina, and the complete metalophid II

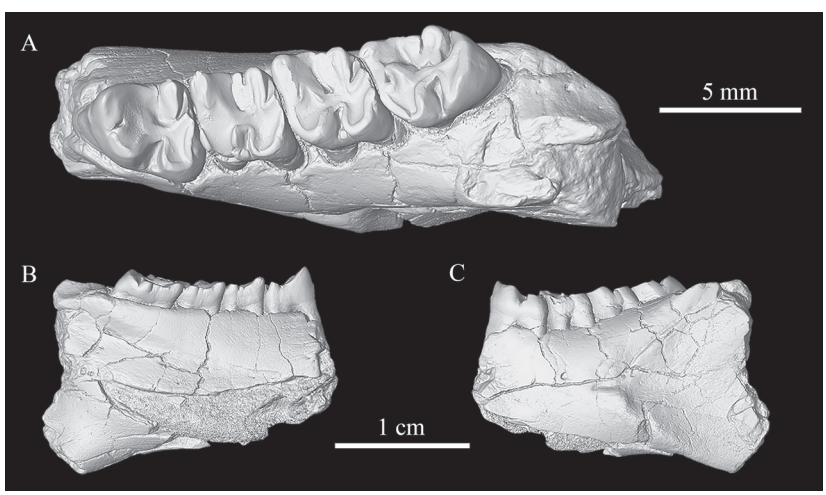

Fig. 2 The right mandible with p4–m3 of *Proardynomys ulausuensis* sp. nov. (IVPP V28608) in occlusal (A), lingual (B) and labial (C) views

on the m3. The new specimen has many features that are similar to *Ardynomys* (Burke, 1936), but there are also many features that are more primitive than those of *Ardynomys*. Compared with *Ardynomys* (Matthew and Granger, 1925; Wood, 1970), the cheek teeth of V28608 have a lower crown, the metaconid is higher than the entoconid, has narrower and less developed lophids, a less expanded hypoconid, and has a lower metasytlid crest on molars. The new specimen from Ula Usu possesses several common features of *Proardynomys*, including a low crown, low and narrow entoconid, wide sinusid, and thin lophid.

Dashzeveg and Meng (1998) first named *Proardynomys* based on materials from the Middle Eocene Mergen locality of the Eastern Gobi, Mongolia. Until now, *Proardynomys* included *P. borkhoii* (Dashzeveg and Meng, 1998) and *Proardynomys* sp. from the "Middle Red" beds of the Erden Obo section, Siziwangqi, Nei Mongol (Li, 2021). The differences between the new specimen and *P. borkhoii* are as following: on the lower cheek teeth of the new specimen, the posterolophid is shorter, the sinusid of p4–m3 is narrower, and the ectostylid is more developed, and the new specimen is smaller than *P. borkhoii* in size (Table 1). The m2 hypolophid of the new specimen is straighter, and the lophids of the m3 are better developed than those in *P. borkhoii*.

Table 1 Measurements of lower cheek teeth of *Proardynomys* (mm)

		P. ulausuensis sp. nov.	*Proardynomys* sp. Li, 2021	*P. borkhoii* Dashzeveg and Meng, 1998	
		V28608	V26554.1–5	PSS 41-30	PSS 41-29
p4	L	3.75		4.10	
	W	3.40		3.00	
m1	L	3.05	3.20–3.30	3.82	3.54
	W	3.10	3.20–3.50	3.44	3.00
m2	L	3.50	3.20–3.50	4.10	3.70
	W	3.25	3.50	3.46	3.14
m3	L	4.00	4.60	4.36	
	W	3.35	3.50	3.45	

The new specimen differs from *Proardynomys* sp. in the Erden obo section in having a smaller size (Table 1), stronger and shorter posterolophid of m1–3, narrower sinusid, more curved hypolophid, and more lingually positioned ectolophid. In addition, the occlusal outline of the m2 of the new specimen is rhombus, while that of *Proardynomys* sp. is trapezoidal. *Proardynomys ulausuensis* sp. nov. is erected for the new specimen.

Ctenodactyloidea Tullberg, 1899

Yuomys Li, 1975

Yuomys cavioides Li, 1975

Specimens IVPP V28604.1, right maxilla with P4–M2; V28604.2, left maxilla with P3–M3; V28604.3, left maxilla with M2; V28604.4, left maxilla with M1–2 and the alveoli of P4–M1; V28604.5, left maxilla with broken P4 and M1–2; V28604.6, left mandible with m2–3; V28604.7, left mandible with m3; V28604.8, left mandible with m2; V28604.9, left M1;

V28604.10–11, right M1s; V28604.12, left M2; V28604.13–15, right M2s; V28604.16–17, left m1s; V28604.18, right m1; V28604.19, left m2; V28604.20–22, right m2s.

Locality and horizon Ula Usu, Erlian Basin, Nei Mongol; the lower part of the Shara Murun Formation.

Measurements see Table 2.

Description and comparisons The tapered P3 has a single root, and a distinct main cusp is on the buccal side (Fig. 3). The P4 is larger than the M1 and has a hypocone that is significantly smaller than the protocone. The metaconule is as large as the metacone located close to the metacone and is free from contact with both the protocone and hypocone. The metaloph is approximately parallel to the protoloph and pointing to the posterior side of the protocone, but not connected to the protocone. The P4 parastyle on the buccal terminal of the anteroloph extends anterolingual-posterolabially and is well-developed but slightly smaller than the paracone. The hypocone of M1–2 is developed and nearly equal in size to the protocone. The M1–2 metaloph connecting the metacone and the metaconule points obliquely to the protocone. Most of the M1s have postparacrista (6/7) and have a very short crest on the anterolingual side of the metaconule that extends to the protocone, but fails to connect the protocone (5/7). The M2 often has a small mesostyle (6/9). The metaloph of the M3 is the more oblique and anterolingually points toward the protocone. The hypocone is also developed on the M3 and separated from the protocone by a shallow cleavage.

Trigonids of m1–2 are higher than talonids (Fig. 3). The metalophid I is complete, the metalophid II is short. The straight hypolophid is well developed, and the mesoconid is absent. The hypoconulid on the posterolingual side of the hypoconid is distinct. The size of the m2

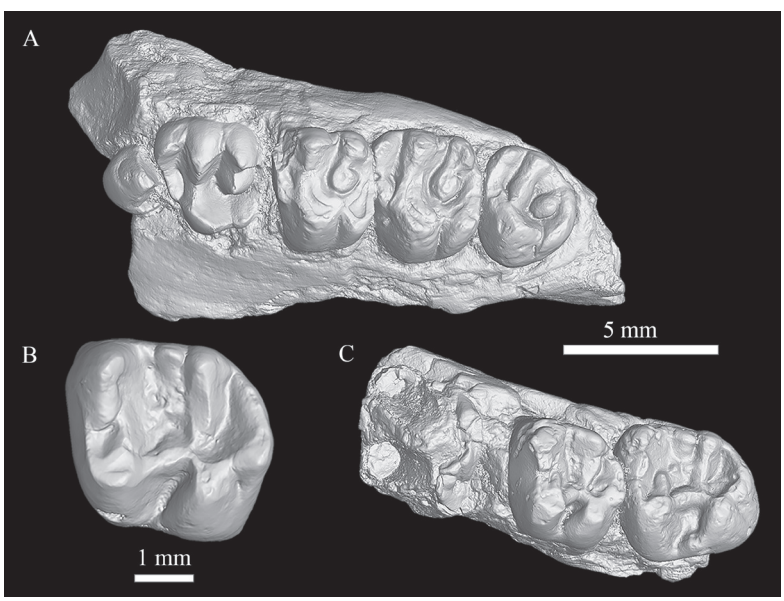

Fig. 3 Cheek teeth of *Yuomys cavioides*
A. IVPP V28604.2, left maxilla with P3–M3; B. V28604.16, left m1; C. V28604.6, left mandible with m2–3

is larger than the m1, the mesostylid of the m2 is more developed than that of the m1, and a conulid (4/6) on the hypolophid is often present on the m2. The m3 has a distinct mesostylid and the posterosinusid is closed (Fig. 3).

Table 2 Measurements of teeth of *Yuomys cavioides* from Ula Usu (mm)

	n	L	Mean	W	Mean
P4	2	3.40–3.60	3.50	3.95	3.95
M1	7	3.20–3.65	3.39	3.10–4.60	3.76
M2	9	3.20–3.75	3.46	3.70–4.40	4.00
M3	1	3.10	3.10	3.80	3.80
m1	3	3.60–3.90	3.73	3.10–3.40	3.23
m2	4	3.60–4.00	3.90	3.70–3.90	3.76
m3	2	4.90–5.00	4.95	3.90–4.30	4.10

The new Ula Usu specimens possess many characters of *Yuomys*, such as a well-developed hypocone that is similar to the protocone in size on M1–2, a distinct metaconule, the metaloph directed toward but not in contact with the protocone on upper molars, and a transverse hypolophid that extends to the ectolophid. *Yuomys* includes ten species: *Y. cavioides* (Li, 1975; Tong, 1997), *Y. eleganes* (Wang, 1978), *Y. minggangensis* (Wang and Zhou, 1982), *Y. weijingensis* (Ye, 1983), *Y. yunnanensis* (Huang and Zhang, 1990), *Y. huangzhuangensis* (Shi, 1989), *Y. huheboerhensis* (Li and Meng, 2015), *Y. altunensis* (Wang, 2017), *Y. magnus* (Li., 2017) and *Y. robustus* (Gong et al., 2021). The new materials are smaller than *Y. altunensis*, *Y. magnus*, *Y. robustus*, and larger than *Y. huheboerhensis* (Fig. 4). The new materials are similar to *Y. eleganes*, but the latter species is different from new materials in that the protoconid and

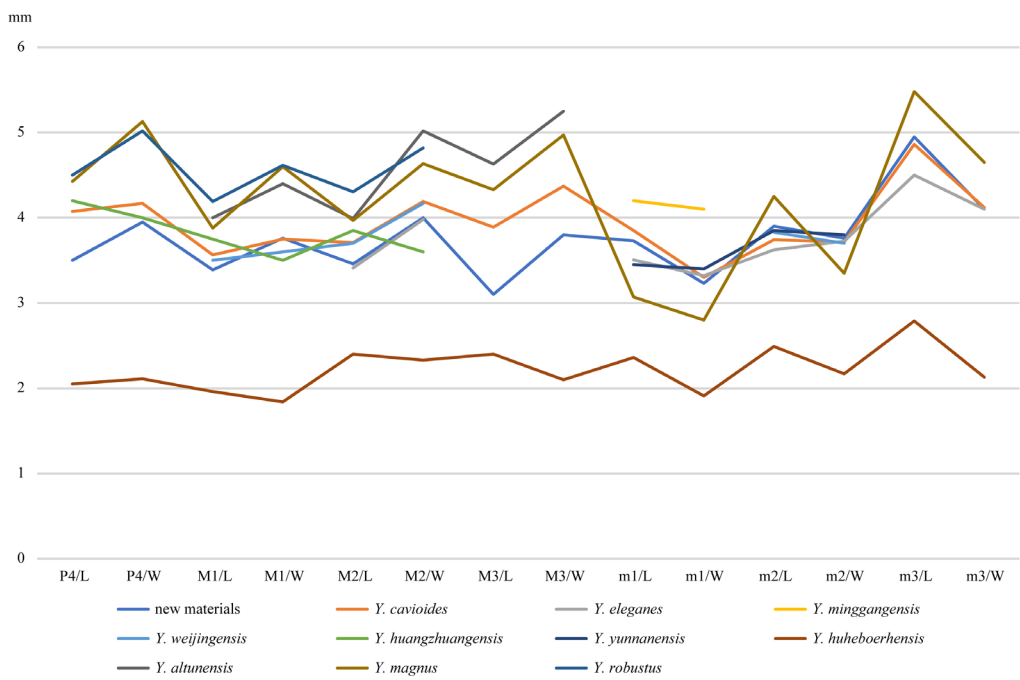

Fig. 4 Diagram of mean measurements of the cheek teeth in ten species of *Yuomys*

the metaconid on the lower teeth are isolated and the conulid on the hypolophid are missing. The size of the new materials falls within the range of variation of *Y. cavioides* and most of the features are identical with those of *Y. cavioides* (Table 2). Compared with the holotype of *Y. cavioides* (V4796.1–4), the hypoconid on the m2 (V28604.6) is larger and the mesostyle on the M2 (V28604.2) is weaker.

Gobiomyidae Wang, 2001

***Gobiomys* Wang, 2001**

***Gobiomys neimongolensis* (Meng et al., 1999)**

Specimens IVPP V28605.1, left M1; V28605.2, right M1; V28605.3, left M2; V28605.4–7, right M2s; V28605.8, left M3; V28605.9, right M3; V28605.10–11, left p4s; V28605.12–16, left m1s; V28605.17–18, right m1s; V28605.19–20, left m2s; V28605.21–22, right m2s; V28605.23–26, left m3s; V28605.27–33, right m3s.

Locality and horizon Ula Usu, Erlian Basin, Nei Mongol; the lower part of the Shara Murun Formation.

Measurements see Table 3.

Description and comparisons The new specimens from Ula Usu possess many common characters with *Gobiomys*, including cheek teeth increasing in size distally, distinct but not swollen main cusps, the P4 is nonmolariform with a weak or absent metaloph, well-developed metaconule of upper molars, lower molars with ectolophid located slightly labially to middle longitudinal line and a narrow sinusid, hypoconulid located at middle of posterior margin of m1–2. *Gobiomys* includes three known species: *G. neimongolensis*, *G. asiaticus* and *G. exiguus* (Meng et al., 1999; Wang, 2001). The new specimens are larger than *G. asiaticus* and *G. exiguus* in size. The Ula Usu specimens differ from *G. asiaticus* in having a weaker anterolophid, thin hypolophid, and well-developed metalophid II on lower molars. They differ from *G. exiguus* in lacking an anteroconid on the p4 and by having the anterolophid and the

Table 3 Measurements of cheek teeth of *Gobiomys neimongolensis* (mm)

		V28605.1–33			V23903.1–44 Li, 2017			V12518.1–34 Wang, 2001		
		n	Range	Mean	n	Range	Mean	n	Range	Mean
M1	L	1	1.50	1.50	13	1.60–1.95	1.73	7	1.53–1.94	1.82
	W	2	1.63–1.77	1.70	13	1.70–2.05	1.82	7	1.70–2.18	1.95
M2	L	5	1.22–1.60	1.49	8	1.75–2.05	1.89	10	1.85–2.30	2.06
	W	5	1.33–1.73	1.55	8	1.95–2.15	2.06	9	2.00–2.46	2.17
M3	L	2	1.40–1.60	1.50	8	1.85–2.10	2.00	5	2.05–2.28	2.19
	W	2	1.45–1.50	1.48	8	1.95–2.25	2.01	5	1.90–2.20	2.08
P4	L	2	1.13–1.20	1.17	1	1.30	1.30	2	1.13–1.17	1.15
	W	2	0.93–1.00	0.97	1	1.20	1.20	2	1.00	1.00
m1	L	7	1.22–1.40	1.30	7	1.50–1.75	1.65	7	1.50–1.90	1.74
	W	7	1.00–1.20	1.11	7	1.34–1.45	1.40	7	1.30–1.63	1.47
m2	L	4	1.53–1.87	1.71	7	1.80–2.00	1.91	12	1.80–2.45	2.04
	W	4	1.30–1.62	1.52	7	1.65–1.75	1.72	14	1.53–2.10	1.81
m3	L	11	1.42–1.83	1.54	11	1.80–2.35	2.12	5	1.91–2.20	2.11
	W	9	1.07–1.45	1.23	11	1.55–1.90	1.71	5	1.42–1.83	1.62

metalophid II on lower molars. The Ula Usu specimens have a M1 with a well-developed metaconule but lack a metaloph, the short metaloph on the M2 and M3, more developed the metalophid II on m1–3, weak or absence of hypolophid, and absence of mesoconid on lower cheek teeth (Fig. 5). All the features are identical with those of *G. neimongolensis*. Compared with the material of *G. neimongolensis* described in Wang (2001) and Li (2017), the size of the new specimens of Ula Usu are slightly smaller (Table 3).

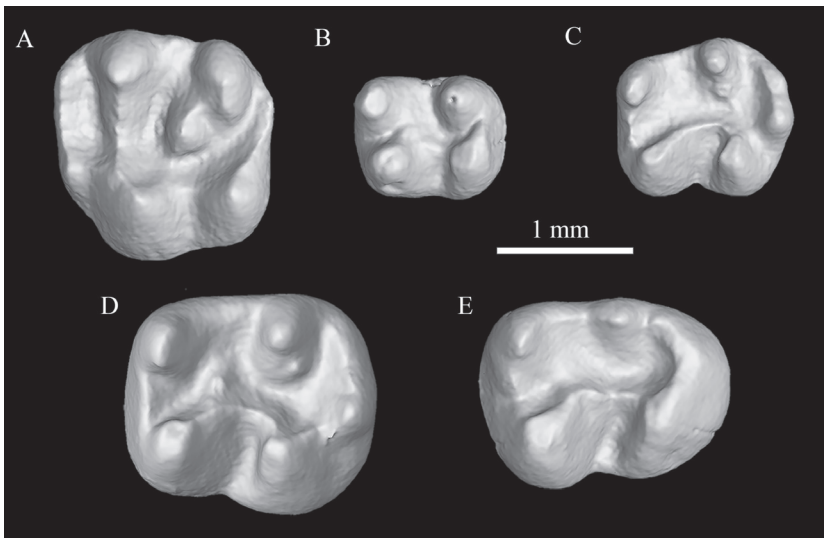

Fig. 5 Cheek teeth of *Gobiomys neimongolensis*
A. IVPP V28605.3, left M2; B. V28605.10, left p4; C. V28605.12, left m1; D. V28605.21, right m2 (reversed); E. V28605.23, left m3

Gobiomys exiguus Wang, 2001

Specimens IVPP V28606.1, right P4; V28606.2–7, right M1s; V28606.8–10, left M2s; V28606.11–17, left M3s; V28606.18–23, right M3s; V28606.24–25, left m1s; V28606.26–28, right m1s; V28606.29–33, right m2s; V28606.34–35, left m3s; V28606.36, right m3.

Locality and horizon Ula Usu, Erlian Basin, Nei Mongol; the lower part of the Shara Murun Formation.

Description and comparisons The new specimens from Ula Usu possess the typical features of *Gobiomys exiguus* (Wang, 2001; Li, 2017) (Table 4) in having the weak entoloph and the strong metaconule on M1–2 and by lacking the anterolophid, hypolophid, and metalophid II on lower molars (Fig. 6). In size, the new specimens are smaller than *G. neimongolensis* and *G. asiaticus*. In morphology, they differ from *G. neimongolensis* and *G. asiaticus* in having a stronger metaconule, less developed metaloph on M1–2 and anterolophid on m1–3, and by lacking a hypolophid and metalophid II on the lower molars. Comparing with *G. exiguus* reported by Wang (2001), the P4 of new specimens lack postparacrista, the hypocone of the M3 is slightly weaker, and the ectolophid of m1–2 is better developed.

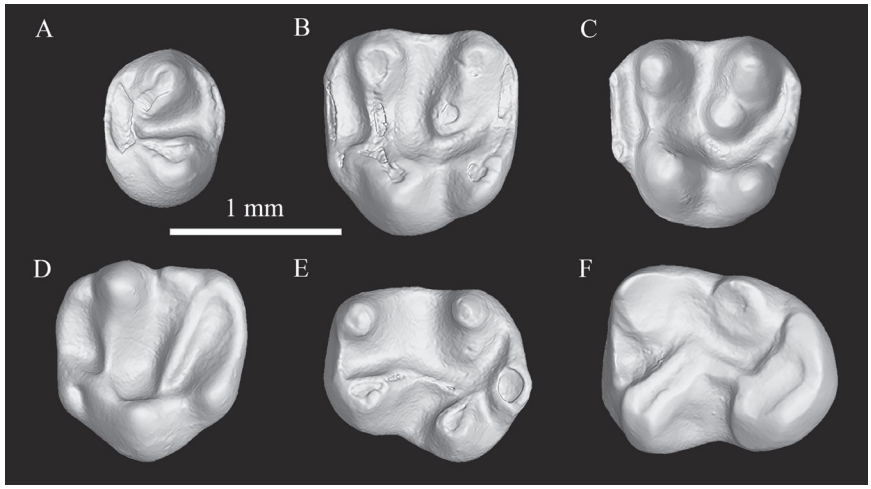

Fig. 6 Cheek teeth of *Gobiomys exiguus*
A. IVPP V28606.1, right P4 (reversed); B. V28606.5, right M1 (reversed); C. V28606.8, left M2; D. V28606.11, left M3; E. V28606.25, left m1; F. V28606.35, left m3

Table 4 Measurements of cheek teeth of *Gobiomys exiguus* (mm)

		V28606.1–36			V23902.1–36 Li, 2017			V12521.1–7 Wang, 2001		
		n	Range	Mean	n	Range	Mean	n	Range	Mean
P4	L	1	0.73	0.73	5	0.05–0.85	0.74	3	0.67–0.8	0.72
	W	1	0.94	0.94	5	0.65–1.2	1.02	3	0.92–1.10	0.99
M1	L	6	1.06–1.20	1.12	13	0.85–1.45	1.15	4	1.00–1.60	1.08
	W	6	1.10–1.20	1.14	13	0.95–1.45	1.20	4	1.0–1.20	1.08
M2	L	2	1.16–1.18	1.17	13	1.05–1.50	1.30	5	1.20–1.38	1.29
	W	2	1.24–1.30	1.27	13	1.10–1.70	1.42	5	1.20–1.40	1.33
M3	L	13	1.15–1.40	1.25	7	1.05–1.45	1.24	3	1.22–1.50	1.34
	W	13	1.21–1.36	1.28	7	1.00–1.50	1.24	3	1.23–1.53	1.35
m1	L	5	1.15–1.24	1.19	6	1.05–1.45	1.21	1	1.27	1.27
	W	5	1.00–1.10	1.04	6	0.90–1.15	1.03	1	1.20	1.20
m2	L	5	1.20–1.30	1.26	7	1.10–1.55	1.32	1	1.34	1.34
	W	5	1.08–1.20	1.15	7	1.10–1.40	1.24	1	1.22	1.22
m3	L	3	1.30–1.44	1.36	5	1.20–1.65	1.40			
	W	3	1.04–1.20	1.13	5	0.90–1.30	1.10			

Gobiomys asiaticus Wang, 2001

Specimens IVPP V28607.1, right P4; V28607.2–5, left M2s; V28607.6–8, right M2s.

Locality and horizon Ula Usu, Erlian Basin, Nei Mongol; the lower part of the Shara Murun Formation.

Description and comparisons Compared to *G. neimongolensis* and *G. exiguus*, the new specimens show some differences including: a smaller metaconule, well-developed metaloph, and weaker entoloph on the upper molars. Compared with the holotype and paratype of *G. asiaticus* (Wang, 2001), the new specimens of Ula Usu are slightly smaller (Table 5) and have a weaker posterior arm of protocone on the P4 and a weaker entoloph on the M2 (Fig. 7).

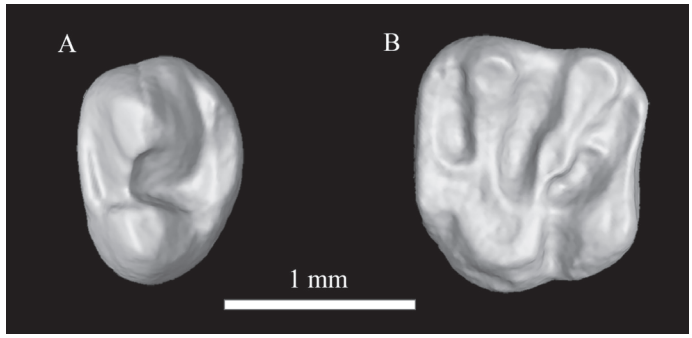

Fig. 7 Upper cheek teeth of *Gobiomys asiaticus*
A. IVPP V28607.1, right P4 (reversed); B. V28607.4, left M2

Table 5 Measurements of the cheek teeth of *Gobiomys asiaticus* (mm)

		V 28607.1-8			V 12524.1-5 Wang, 2001		
		n	Range	Mean	n	Range	Mean
P4	L	1	0.86	0.86	1	0.95	0.95
	W	1	1.28	1.28	1	1.40	1.40
M2	L	7	1.20–1.56	1.30	1	1.53	1.53
	W	7	1.20–1.58	1.37	1	1.77	1.77

Cricetidae Fischer von Waldheim, 1817

Pappocricetodon Tong, 1992

Pappocricetodon rencunensis Tong, 1992

Specimens IVPP V28610.1, a right mandible with m2–3; V28610.2–6, left M1s; V28610.7–9, right M1s; V28610.10–12, left M2s; V28610.13–18, right M2s; V28610.19, right M3; V28610. 20–26, left m1s; V28610.27–36, right m1s; V28610.37–39, right m2s; V28610.40–42, left m3s.

Locality and horizon Ula Usu, Erlian Basin, Nei Mongol; the lower part of the Shara Murun Formation.

Description and comparisons The new specimens from Ula Usu possess many characters in common with *Pappocricetodon* (Tong, 1992), such as the brachyodont cheek teeth, an obvious mesoloph on the upper cheek teeth, a bulbous protocone on M1–3, the M1 has a small anterior lobe, low anterocone, a long anterolophule extending to the anterocone, a weak ectomesolophid on m1–3, a m1 with a small anteroconid, and a metalophid II that connects to the middle part of the anterior arm of the protoconid on m2–3 (Fig. 8). *Pappocricetodon* contains 6 species: *P. rencunensis*, *P. antiquus*, *P. neimongolensis*, *P. schaubi*, *P. siziwangqiensis*, and *P. kazakstanicus* (Wang et al., 2020). Comparing with *P. antiquus* (Wang and Dawson, 1994) and *P. kazakstanicus* (Emry et al., 1998), the anterior lobe and anterocone on the M1 of the new specimens is larger, and the ectomesolophid on the lower molars is present. And the mesoloph on M1–2 of the new specimens is shorter than that of *P. kazakstanicus*. The new specimens are smaller than *P. kazakstanicus*, *P. antiquus* and *P.*

schaubi (Zdansky, 1930; Tong, 1997; Li, 2018). They differ from *P. schaubi* in having a smaller anterior lobe and a lower anterocone on the M1 as well as a smaller anteroconid and a weaker mesoconid on the m1. *Pappocricetodon siziwangqiensis* (Li et al., 2016) differs from the new specimens by having a protoloph that is connected to the posterior side of paracone on the M1 and in lacking the contact facet at the anterior surface on the M1 (absence of premolar). The new specimens differ from *P. neimongolensis* (Li, 2012) in having larger anterocones and more developed mesolophs on the M1 and M2, a narrower anterior groove and mesosinus on the M3, a larger anteroconid on the m1, a longer and more complete metalophid I, and a less developed mesolophid and ectomesolophid on the m2. The new specimens from Ula Usu have

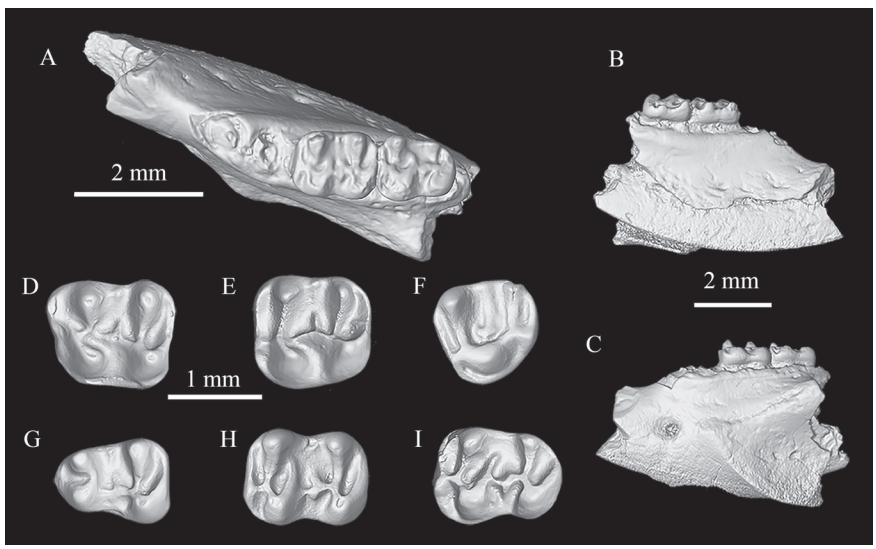

Fig. 8 Mandible and cheek teeth of *Pappocricetodon rencunensis*
A–C. IVPP V28610.1 in occlusal (A), lingual (B), and labial (C) views of the right mandible with m2–3 (reversed); D. V28610.2, left M1; E. V28610.11, left M2; F. V28610.19, right M3 (reversed); G. V28610.20, left m1; H. V28610.37, right m2 (reversed); I. V28610.42, left m3

Table 6 Measurements of molars of *Pappocricetodon rencunensis* (mm)

		V28610.1–42			V10288.1–378 Tong, 1997		
		n	Range	Mean	n	Range	Mean
M1	L	8	1.35–1.62	1.46	62	1.30–1.65	1.47
	W	8	1.13–1.25	1.17	62	0.95–1.25	1.33
M2	L	9	1.22–1.40	1.31	76	1.10–1.50	1.34
	W	8	1.04–1.27	1.18	74	1.00–1.33	1.20
M3	L	1	1.10	1.10	56	0.95–1.25	1.10
	W	1	1.10	1.10	58	1.00–1.25	1.11
m1	L	16	0.98–1.35	1.17	50	1.15–1.45	1.31
	W	14	0.71–1.02	0.87	51	0.85–1.10	0.97
m2	L	3	1.24–1.33	1.29	53	1.20–1.57	1.41
	W	3	1.02–1.10	1.06	53	0.95–1.25	1.10
m3	L	4	1.29–1.36	1.32	42	1.20–1.50	1.40
	W	4	1.00–1.15	1.07	41	0.95–1.20	1.10

a developed mesostyle and mesoloph on the upper molars, a small anterocone, a low anterior lobe, a developed anterolophule that connects to the anterocone on the M1, the less developed hypocone and metacone on the M3, a narrow trigonid, a complete metalophid II on m1–3, and a developed ectomesolophid on the m1. All the features are identical to those of *P. rencunensis* (Tong, 1992, 1997). The size of the new specimens falls within the range of variation of *P. rencunensis* (Tong, 1992, 1997) (Table 6).

Dipodidae Fischer von Waldheim, 1817

***Allosminthus* Wang, 1985**

***Allosminthus uniconjugatus* (Tong, 1997)**

Banyuesminthus uniconjugatus Tong, 1997

Allosminthus uniconjugatus Wang, 2008

Specimens IVPP V28611.1–2, left M1s; V28611.3–6, right M1s; V28611.7–8, left M2s; V28611.9, left M3; V28611.10, right M3; V28611.11–13, left m1s; V28611.14–21, left m2s; V28611.22–31, right m2s; V28611.32–33, left m3s; V28611.34–35, right m3s.

Locality and horizon Ula Usu, Erlian Basin, Nei Mongol; the lower part of the Shara Murun Formation.

Description and comparisons Wang (1985) named *Allosminthus* based on specimens from Qujing in Yunnan, which was later revised by Wang (2008), Daxner-Höck (2001) and Daxner-Höck et al. (2014). Until now, *Allosminthus* has included six species: *A. ernos* (Wang, 1985), *A. majusculus* (Wang, 1985), *A. diconjugatus* (Tong, 1997), *A. uniconjugatus* (Tong, 1997), *A. minutus* (Daxner-Höck, 2001; Daxner-Höck et al., 2014) and *A. khandae* (Daxner-Höck, 2001).

The new specimens from Ula Usu are smaller than *A. majusculus*, *A. diconjugatus*, and *A. ernos*, but larger than *A. khandae* and *A. minutus*. It differs from *A. diconjugatus* in lacking protoloph II and the posterior arm of the protocone on the M1, and lacking a distinct mesolophid on the m1 (Fig. 9). *Allosminthus majusculus* differs from the new specimens in having a smaller anteroconid and a stronger hypolophid on the m1, a closed trigonid and a more developed ectomesolophid on the m2. The specimens from Ula Usu differ from *A. khandae* and *A. minutus* in having a weaker entoloph on the M2, a more complete metalophid II on m2–3, and by lacking the metalophid I on m2–3 (Fig. 9). Compared with *A. ernos* (Wang, 1985), the new specimens lack a complete entoloph on the M1, and have the thin hypolophid and anterior arm of the hypoconid on the m1.

The materials from the Ula Usu share the following features with *A.uniconjugatus*: a strong anterior arm of the protocone which connects with the paracone on the M1, no protoloph II and the weak posterior arm of the protocone on the M1, the metaloph connecting the metacone and anterior arm of the hypocone on M2–3, and the complete hypolophid on m1–2. Compared to the holotype of *A. uniconjugatus* (Tong, 1997) from the Rencun Member of the Hedi Formation of Henan Province (Table 7), the metaloph on the M1 from the Ula Usu is shorter and connected to the anterior arm of the hypocone (4/6) or does not reach to the hypocone (2/6), and the protoconid on the m2 is smaller.

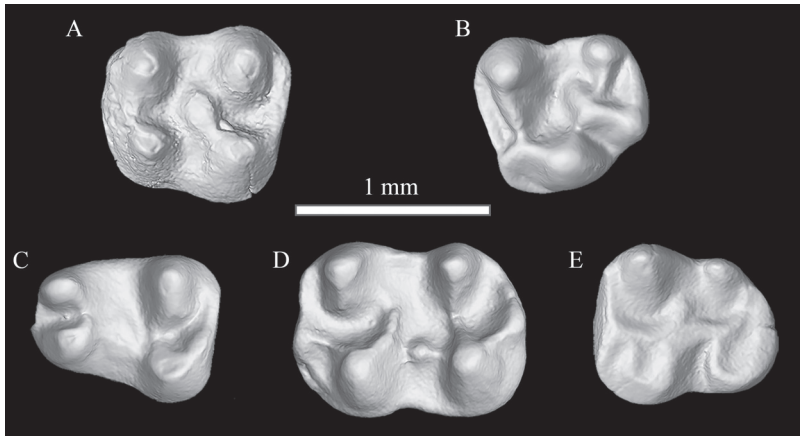

Fig. 9 Selected molars of *Allosminthus uniconjugatus*
A. IVPP V28611.5, right M1 (reversed); B. V28611.10, right M3 (reversed); C. V28611.12, left m1; D. V28611.15, left m2; E. V28611.35, right m3 (reversed)

Table 7 Measurements of molars of *Allosminthus uniconjugatus* (mm)

		V28611.1–35			V10298.1–17 Tong, 1997		
		n	Range	Mean	n	Range	Mean
M1	L	6	0.93–1.07	1.01	2	1.13–1.20	1.17
	W	5	0.75–0.95	0.88	2	0.97–1.03	1.00
M2	L	2	0.95–0.97	0.96	3	1.03–1.10	1.07
	W	2	0.80–0.87	0.84	3	0.95–1.00	0.97
M3	L	2	0.85–0.87	0.86	2	0.83	0.83
	W	2	0.81–0.84	0.83	2	0.83–0.87	0.85
m1	L	3	0.96–1.04	1.00	2	1.07–1.10	1.09
	W	3	0.78–0.84	0.80	2	0.84–0.87	0.86
m2	L	18	1.02–1.20	1.13	3	1.03–1.10	1.07
	W	18	0.80–0.95	0.88	2	0.80–0.87	0.84
m3	L	4	0.94–1.02	0.96	3	0.97–1.03	1.01
	W	4	0.75–0.87	0.80	3	0.88–0.90	0.89

Primisminthus Tong, 1997

Primisminthus shanghenus Tong, 1997

Specimens IVPP V28612.1–3, left M1s; V28612.4–5, right M1s; V28612.6–11, left M2s; V28612.12–17, right M2s.

Locality and horizon Ula Usu, Erlian Basin, Nei Mongol; the lower part of the Shara Murun Formation.

Description and comparisons The new specimens have a trapezoidal M1 and rectangular M2 in occlusal outline, no protoloph II and a lophate metacone on M1–2, a complete protoloph I (which connects the paracone and protocone), a long anterior arm of hypocone connecting to mesocone, and a short metaloph which extends to the anterior arm of hypocone or connects to the mesocone on the M1, and a more developed posterior arm of the protocone on the M2 (Fig. 10). All the features are identical with those of *Primisminthus*

shanghenus (Tong, 1997). Compared to the type specimens of *P. shanghenus* from the Rencun Member of the Hedi Formation of Henan, the size of the specimens reported here are slightly larger (Table 8), the mesoloph of the M1 is thinner, and the posterior arm of the protocone on the M2 is better developed. The new specimens differ from those of *A. uniconjugatus* from the same horizon of Ula Usu in having the tapered main cusps on the upper molars and the stronger posterior arm of the protocone on the M2.

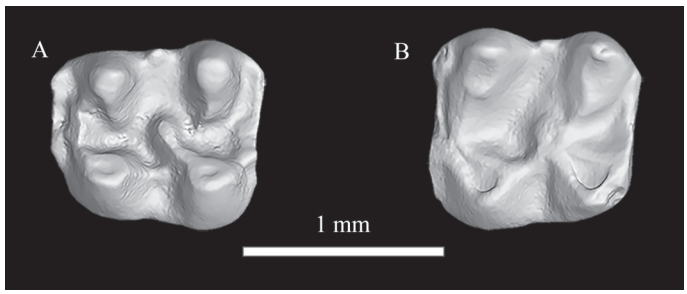

Fig. 10 Upper molars of *Primisminthus shanghenus*
A. IVPP V28612.1, left M1; B. V28612.10, left M2.

Table 8 Measurements of molars of *Primisminthus shanghenus* (mm)

		V28612.1–17			V10295.1–15 Tong, 1997		
		n	Range	Mean	n	Range	Mean
M1	L	5	0.99–1.07	1.05	2	0.90–1.00	0.95
	W	5	0.86–0.98	0.93	2	0.75–0.90	0.83
M2	L	12	0.91–1.18	1.06	7	0.95–1.00	0.97
	W	12	0.85–1.11	0.99	7	0.90–0.95	0.91

Ischyromyidae Alston, 1876

Hulgana Dawson, 1968

Hulgana cf. *H. ertnia* Dawson, 1968

Specimens IVPP V28609.1, right P4; V28609.2–5, left M1s; V28609.6–10, right M1s; V28609.11–12, left M2s; V28609.13, left M3; V28609.14, right dp4; V28609.15–17 left p4s; V28609.18–19, right p4s; V28609.20, right m1; V28609.21–22, right m2s; V28609.23, right m3.

Locality and horizon Ula Usu, Erlian Basin, Nei Mongol; the lower part of the Shara Murun Formation.

Description and comparisons The upper cheek teeth have a simple crown structure with either a small hypocone or none at all and no conules or styles. On the P4, the protocone, paracone, and metacone are prominent, while it lacks a hypocone. The complete protoloph and metaloph separately extend from the lingual side of the paracone and metacone, and all make contact with the labial side of the protocone. The protoloph is slightly curved and the metaloph is straight. The anteroloph connects to the paracone, and it is lower and narrower than that of the M1.

The M1 is nearly square in occlusal view. The M1 is larger than the P4. The M1

has distinct paracone, metacone, protocone, and no independent hypocone. The metacone is slightly larger than the paracone. The straight protoloph and the curved metaloph are separately connected to the labial side of the protocone. The centrocrista between the paracone and metacone is concave (Fig. 11). The crown of M2 is narrower than that of the M1. The metacone is slightly smaller than the paracone and the centrocrista is low. The anteroloph is longer and narrower than that of the M1 (Fig. 11). The M3 is smaller than M1–2. The metacone is very low and small. The protoloph is straight and the metaloph is short (Fig. 11).

The p4 is slightly narrower anteriorly than posteriorly and is smaller than the lower molars. The hypoconid extends anterolabially. On the p4, the metalophid I is missing, the metalophid II is complete, the ectolophid is short, the hypolophid is absent, and the deep sinusid opens anterolabially. The posterolophid connects to the entoconid and sometimes multiple conules are present on the posterolophid (4/5) (Fig. 11).

V28609.14 is noticeably smaller than the p4. The metalophid I is complete and the trigonid opens posteriorly. Compared with the p4, the ectolophid of V28609.14 is stronger and the sinusid is shallower and wider. The distinct hypoconulid is present on the posterolophid (Fig. 11). Based on the above characteristics, it is tentatively considered to be a dp4.

The m1 is rhomboidal in occlusal view. The prominent protoconid, metaconid, hypoconid, and entoconid are on the edge of the crown of the lower molars and they surround a big mesosinusid (talonid basin). The entoconid is weaker than the protoconid and the metaconid. The trigonid is slightly wider than the talonid. The metalophid I is straight and the metalophid II is short and does not connect to the metaconid on m1–3. The m2 is larger than the m1. The posterior end of the m3 is rounded (Fig. 11).

The new specimens from the Ula Usu are similar to *Hulgana ertnia* from the Jhama Obo,

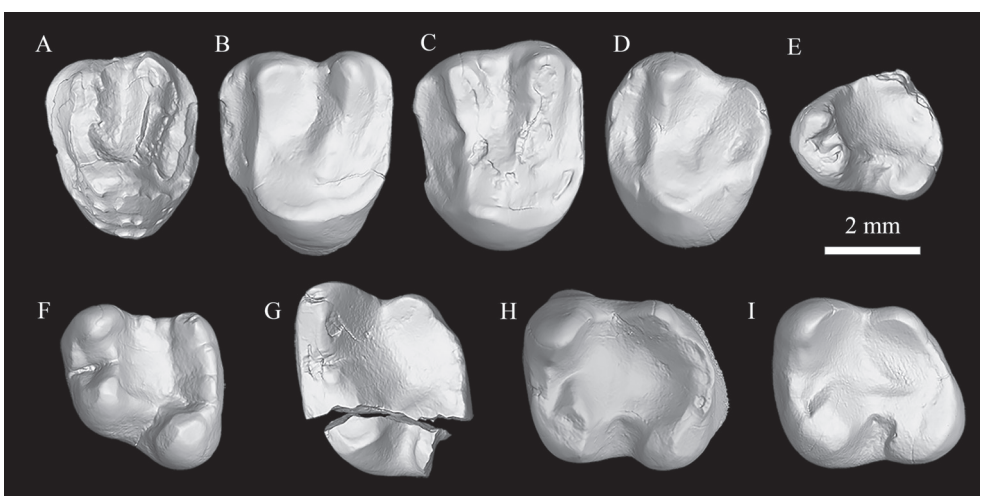

Fig. 11 Cheek teeth of *Hulgana* cf. *H. ertnia*
A. IVPP V28609.1, right P4 (reversed); B. V28609.3, left M1; C. V28609.12, left M2; D. V28609.13, left M3; E. V28609.14, right dp4 (reversed); F. V28609.15, left p4; G. V28609.20, right m1 (reversed); H. V28609.21, right m2 (reversed); I. V28609.23, right m3 (reversed)

Nei Mongol (Dawson, 1968) because they have the well-developed anteroloph and posteroloph, no independent hypocone, no conules on P4–M3, the main cusps on the edge of the crown of lower molars, wide mesosinusid, and no mesostylid or hypolophid on the lower teeth.

The new materials differ from *H. ertnia* in having a smaller size (Table 9), a longer and straighter protoloph and a shorter and more curved metaloph on the P4, the multiple hypoconulids on the posterolophid of lower cheek teeth, and a shorter m3. We regard the new specimens as *Hulgana* cf. *H. ertnia*. The M3 and dp4 of *Hulgana* are reported herein for the first time.

Table 9 Measurements of cheek teeth of *Hulgana* cf. *H. ertnia* and *H. ertnia* (mm)

		Hulgana cf. *H. ertnia* V28609.1–23			*H. ertnia* AMNH 26085–26088 Dawson, 1968		
		n	Range	Mean	n	Range	Mean
P4	L	1	3.15	3.15	2	3.50–3.90	3.70
	W	1	3.85	3.85	2	4.60–4.80	4.70
M1	L	7	3.40–3.70	3.53	2	4.10–4.40	4.25
	W	7	3.75–4.75	4.14	2	4.80	4.80
M2	L	2	3.35–3.55	3.45	2	3.70–3.90	3.80
	W	1	4.45	4.45	2	5.00–5.20	5.10
M3	L	1	3.40	3.40			
	W	1	4.00	4.00			
dp4	L	1	3.20	3.20			
	W	1	2.60	2.60			
p4	L	3	3.50–3.95	3.65	1	3.90	3.90
	W	4	3.00–3.40	3.18	1	3.90	3.90
m1	L	1	—	—	2	3.70–4.20	3.95
	W	1	—	—	2	3.90–4.30	4.10
m2	L	2	4.15–4.20	4.18	2	3.90–4.30	4.10
	W	2	3.75	3.75	2	4.10–4.40	4.25
m3	L	1	4.20	4.20	1	4.80	4.80
	W	1	3.50	3.50	1	4.60	4.60

5 Discussion and conclusion

5.1 The Sharamurunian rodent fauna in the Erlian Basin

The rodent materials from the middle Eocene Sharamurunian in Ula Usu of the Erlian Basin include the ctenodactyloids *Yuomys cavioides*, *Gobiomys neimongolensis*, *G. exiguus*, and *G. asiaticus*, the cricetid *Pappocricetodon rencunensis*, the ischyromyid *Hulgana* cf. *H. ertnia*, the cylindrodontid *Proardynomys ulausuensis*, and the dipodids *Allosminthus uniconjugatus* and *Primisminthus shanghenus*. These specimens are referred to 9 species belonging to 7 genera, 4 families, and 1 superfamily of Rodentia. These fossils represent the best-known Sharamurunian rodent assemblages with a high species diversity in the Erlian Basin.

In the Erlian Basin, the mammal taxa from the “Lower Red” beds of the Erden Obo, Nomogen, Siziwangqi indicate that the age of the horizon is correlative to the Sharamurunian (Fostowicz-Frelik et al., 2012, 2015; Li, 2018), and rodent fossils from the “Lower Red” beds of the Erden Obo have been studied in detail (Li, 2017, 2018, 2021). There is a smaller number

of rodent fossils and lower generic richness in the "Lower Red" beds of the Erden Obo than in Ula Usu, but the rodents that were found from the "Lower Red" beds of the Erden Obo, such as the ctenodactyloids *Gobiomys* and *Yuomys* as well as the dipodids *Allosminthus* and *Primisminthus*, are also present in the rodent fauna of Ula Usu. The rodent assemblages from both localities have similar characteristics.

Due to the facts that the rodent assemblages from Ula Usu and the "Lower Red" beds of the Erden Obo have similar characteristics and both localities are in the same basin, we selected rodent fossils from the above two sites to comprehensively analysis the Sharamurunian rodent fauna in the Erlian Basin. The approximately 248 rodent specimens collected from the Ula Usu locality and the "Lower Red" beds of the Erden Obo in the Erlian Basin represent at least 67 individuals counted by the minimum number of individuals (MNI) (Table 10).

Based on the MNI, ctenodactyloids are the dominant elements (constituting 47.76% of the total) and they include 5 species of 2 genera. The diversity and proportion of *Gobiomys* is higher than these of *Yuomys*. Dipodids include *Allosminthus uniconjugatus* and *Primisminthus shanghenus* and they occupy 26.87% and are the second most dominant group. The cricetid *Pappocricetodon rencunensis* and the ischyromyid *Hulgana* cf. *H. ertnia* occupy 14.93% and 7.46%, respectively. The cylindrodontids occupy less than 3% and has a low level of diversity in the Sharamurunian rodent fauna in Erlian Basin.

5.2 Comparison with the Irdinmanhan and the Ulangochuian rodent fauna

Romer (1966) proposed some related Asian Paleogene Land Mammal Ages (APLMA) based on mammalian faunas from the Mongolian Plateau. Thereafter, the age and name of the APLMA were revised by different researchers, and these land mammal ages have often been used in the discussion of intercontinental biostratigraphical correlation and mammalian dispersals (Li and Ting, 1983; Tong et al., 1995; Wang, 1997a, b; Wang et al., 2012, 2019). Now the Bumbanian, Arshantan, Irdinmanhan, Sharamurunian, Ulangochuian, and Ergilian ages in the Eocene have been widely adopted as the Asian Paleogene Land Mammal Ages in

Table 10 Relative abundance of fossil rodents of the Sharamurunian rodent fauna in the Erlian Basin

Superfamily or family	Species	TNS	MNI	PES (%)	PEF (%)
Ctenodactyloidea	*Yuomys cavioides*	22 (A, 22)	5 (A, 5)	7.46%	47.76%
	Yuomys magnus	15 (B, 15)	5 (B, 5)	7.46%	
	Gobiomys neimongolensis	34 (A, 33; B, 1)	8 (A, 7; B, 1)	11.94%	
	Gobiomys exiguus	48 (A, 36; B, 12)	10 (A, 7; B, 3)	14.93%	
	Gobiomys asiaticus	8 (A, 8)	4 (A, 4)	5.97%	
Ischyromyidae	*Hulgana* cf. *H. ertnia*	23 (A, 23)	5 (A, 5)	7.46%	7.46%
Cylindrodontidae	*Proardynomys ulausuensis*	1 (A, 1)	1 (A, 1)	1.49%	2.98%
	Gobiocylindrodon sp.	1 (B, 1)	1 (B, 1)	1.49%	
Cricetidae	*Pappocricetodon rencunensis*	42 (A, 42)	10 (A, 10)	14.93%	14.93%
Dipodidae	*Allosminthus uniconjugatus*	36 (A, 35; B, 1)	11 (A, 10; B, 1)	16.42%	26.87%
	Primisminthus shanghenus	18 (A, 17; B, 1)	7 (A, 6; B, 1)	10.45%	

MNI: minimum number of individuals; PEF: percentage of each family (superfamily) in the rodent fauna; PES: percentage of each of the species in the rodent fauna; TNS: total number of specimens. A, based on the specimens from the Ula Usu. B, based on the specimens from the "Lower Red" beds of the Erden Obo.

the Geologic Time Scales (Luterbacher et al., 2004; Vandenberghe et al., 2012; Speijer et al., 2020). In order to better understand the characteristics of the Sharamurunian rodents as well as the evolution and turnovers of rodent faunas in the Erlian Basin, we compared this rodent fauna to the adjacent Irdinmanhan and Ulangochuian rodent faunas in detail.

In the Erlian Basin, the Irdinmanhan rodents were recorded from the lower part of the Irdin Manha Formation in the Nuhetingboerhe-Huheboerhe area (Wang et al., 2010; Li and Meng, 2015; Li, 2016) and the middle part of the "Basal White" beds of the Erden Obo (Li, 2017, 2018, 2021; Li et al., 2017). The compositions of the Sharamurunian and Irdinmanhan rodent faunas are similar at the family level, but they differ in their generic composition (Fig. 12). Ctenodactyloids are dominant in both the Sharamurunian and Irdinmanhan rodent faunas, but the species richness of ctenodactyloids obviously declined and the proportion of ctenodactyloids dropped from 65.76% to 47.76% in the rodent fauna from the Irdinmanhan to Sharamurunian. The ctenodactyloids show a distinct substitution. *Tamquammys*, *Simplicimys* and *Yongshengomys* were abundant during the Irdinmanhan, but they did not survive into the Sharamurunian. Instead, *Gobiomys* became the dominant ctenodactyloid during the Sharamurunian. Although the genus *Yuomys* appeared in both the Irdinmanhan and Sharamurunian rodent faunas, but it is represented by different species. The cricetid *Pappocricetodon* was present in both the Irdinmanhan and Sharamurunian rodent faunas, but its proportion in the Irdinmanhan is slightly higher than that in the Sharamurunian. *Pappocricetodon neimongolensis* (Li, 2012; Li et al., 2017) from the Irdinmanhan fauna is more primitive than *P. rencunensis* (Tong, 1992, 1997) of the Sharamurunian fauna. Both the species richness and proportion of ischyromyids declined from the Irdinmanhan to the Sharamurunian rodent faunas. Dipodids and cylindrodontids were absent in the Irdinmanhan rodent fauna, but dipodids were present and became the second most dominant element (26.87%) in the Sharamurunian rodent fauna. The cylindrodontids *Proardynomys ulausuensis* and *Gobiocylindrodon* sp. were also present.

Plenty of Ulangochuian rodents in the Erlian Basin were reported from the "Lower White" to the "Middle White" beds of the Erden Obo section (Li, 2018, 2020, 2021). The Ulangochuian rodent fauna consisted of ctenodactyloids, cricetids, dipodids, and cylindrodontids. Compared to the Sharamurunian rodents, the genera richness and abundance of the cricetids and dipodids of the Ulangochuian rodents increased significantly. Cricetids (5 species of 3 genera) and dipodids (4 species of 2 genera) became the dominant elements in the Ulangochuian rodent fauna (Fig. 12). Although the cricetid *Pappocricetodon* and the dipodid *Allosminthus* were present in both the Sharamurunian and the Ulangochuian rodent faunas, they are represented by different species. From the Sharamurunian to Ulangochuian, the proportion of ctenodactyloids in the rodent faunas declined and the generic richness decreased to two genera (*Gobiomys* and *Yuomys*). In addition, ischyromyids were present in the Sharamurunian fauna, but they were absent in the Ulangochuian fauna. The generic richness of Ulangochuian cylindrodontids is slightly higher than that in the Sharamurunian.

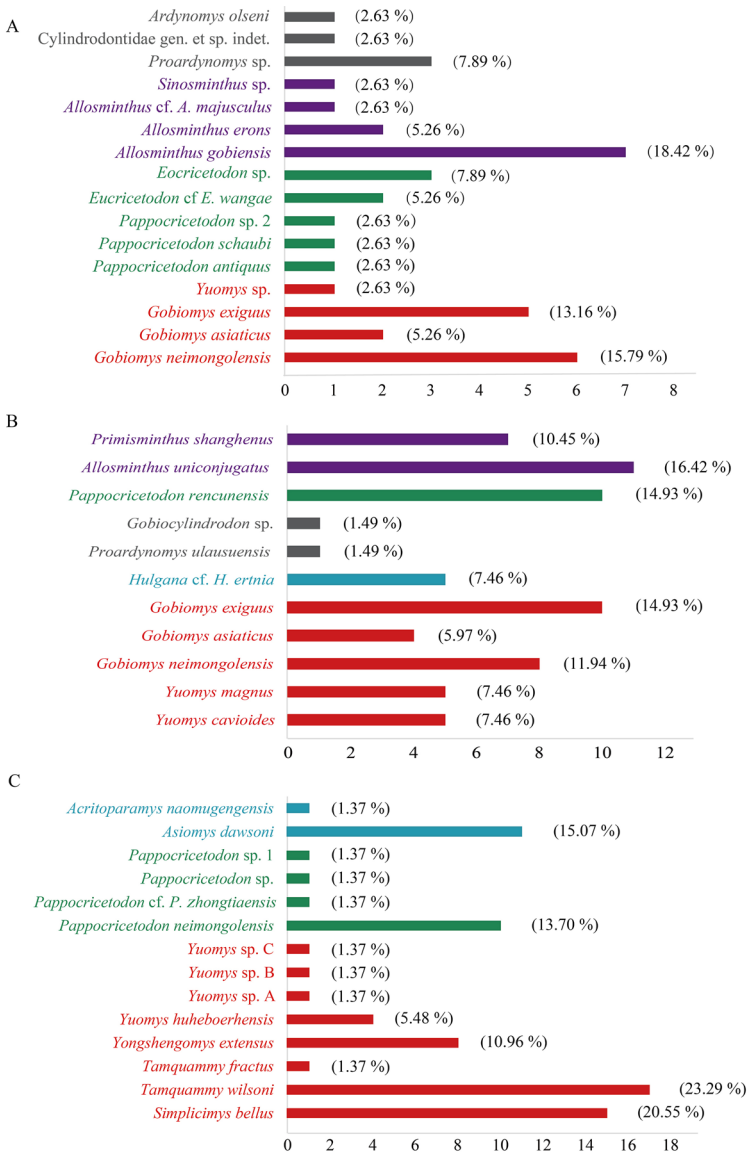

Fig. 12 Percentage chart of the rodent assemblage compositions of the Ulangochuian (A), Sharamurunian (B), and Irdinmanhan (C) rodent faunas in the Erlian Basin, by minimum number of individuals
The ctenodactyloids are represent by red, cricetids by green, ischyromyids by blue, dipodids by purple, and cylindrodontids by gray. The numbers on the horizontal axis are the minimum number of individuals and the numbers in brackets represent its percentage in the fauna

5.3 The evolution and turnovers of rodent faunas in the Erlian Basin

The Erlian Basin is an important Asian Paleogene fossil producing area, and the Tertiary beds in the Erlian Basin were first explored by the Central Asiatic Expeditions (CAE) in the 1920s (Granger and Berkey, 1922; Berkey and Granger, 1923; Matthew and Granger, 1926). Since the investigations of the CAE, numerous fossils have been collected from the Erlian Basin, but rodents and other micromammals were rare. During the past two decades, the IVPP

has led a comprehensive investigation in the Erlian Basin that included lithostratigraphy, biostratigraphy, and paleomagnetic research. Thousands of teeth, numerous maxilla, and jaw fragments of rodents have been collected and systematically reported (Wang, 2001, 2007; Wang et al., 2010; Li and Meng, 2015; Li, 2012, 2016, 2017, 2018, 2020, 2021; Li et al., 2016, 2017, 2019). These rodents are distributed in different layers and assemblages which has provided important evidence for stratigraphic division as well as for the lithological and biostratigraphic correlations (Li, 2016; 2018). A partial rodent sequence in the Erden Obo section of the Erlian Basin has been established, and the rodent assemblages show a transformation (Li, 2018).

We counted the rodent fossils from the Erlian Basin and analyze their species richness per family (Figs. 13, 14) following the Asian Paleogene Land Mammal Ages framework (Speijer et al., 2020). In the Bumbanian age of the early Eocene, the ctenodactyloids had a relatively high diversity. From the Bumbanian to the Irdinmanhan, the species richness of ctenodactyloids continuously increased. Cricetids and dipodids first appeared Irdinmanhan and Sharamurunian ages, separately. Since the Sharamurunian age, the species richness of ctenodactyloids was reduced, whereas that of cricetids and dipodids distinctly increased from the Ulangochuian. Based on the numbers of species, it is evident that the rodent faunas of the Erlian Basin changed from ctenodactyloid dominant assemblages during the Bumbanian to the Sharamurunian ages, to the cricetid and dipodid dominant assemblages during the Ulangochuian and the Ergilian (Fig. 13).

Furthermore, the early Oligocene strata in the Erlian Basin were discontinuous and the rodent fossils from these strata were limited. Although the known early Oligocene rodent fossils reveal the differences between those Eocene assemblages, discussing this change through the Eocene-Oligocene boundary is beyond the scope of this study.

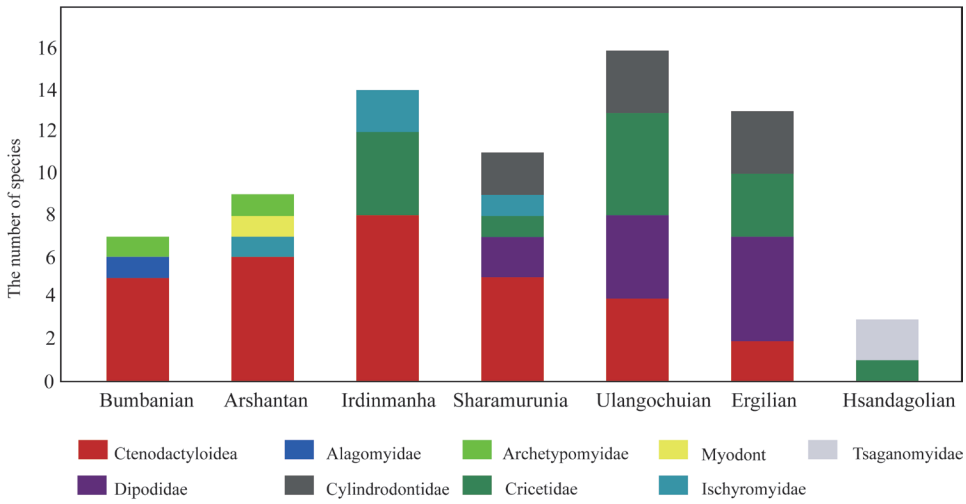

Fig. 13 The species richness per each family of the rodent faunas in the Erlian Basin from the Bumbanian to the Hsandagolian

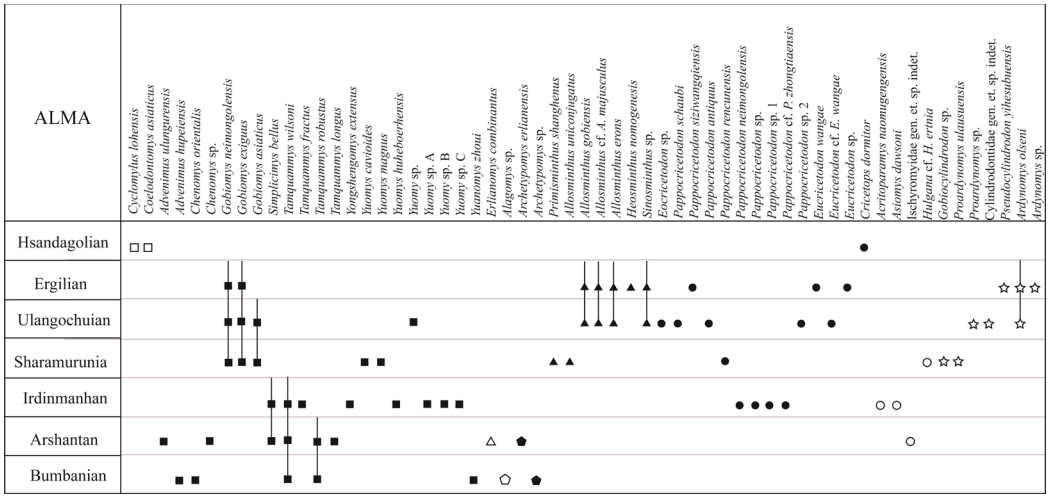

Fig. 14 Stratigraphic distribution of rodent taxa in the Erlian Basin

Considering that it involves multiple localities in the Erlian Basin, the figure can only represent the occurrences of a species in the ALMA, but do not give precisely the specific formation that yielded them Ctenodactyloidea is figured as a black square, Tsaganomyidae as a hollow square, Dipodidae as a black triangle, Myodont as a hollow triangle, Cricetidae as a black circle, Ischyromyidae as a hollow circle, Archetypomyidae as a black pentagon, Alagomyidae as a hollow pentagon, and Cylindrodontidae as a hollow star. ALMA: Asian Land Mammal Age

5.4 Comparison with the Shanghe-Zhaili fauna in the Yuanqu Basin, Shanxi

Except for the Erlian Basin of Nei Mongol, the Shanghe-Zhaili in the Yuanqu Basin of Shanxi is another important Sharamurunian fossil producing area in China. Rodent fossils from the Yuanqu Basin are also abundant and have been studied using the MNI (Tong, 1997). The rodent faunas from the Erlian Basin and the Yuanqu Basin are similar, and rodents in both sites share ctenodactyloids, cricetids, dipodids and ischyromyids, even some of same genera and species, such as ctenodactyloid *Yuomys cavioides*, cricetid *Pappocricetodon rencunensis*, and the dipodids *Allosminthus uniconjugatus* and *Primisminthus shanghenus* (Table 11). However, there are also differences between the two rodent faunas. The rodent species richness from the Yuanqu Basin is slightly higher than that in the Erlian Basin. Ctenodactyloids are the dominant group in the Sharamurunian rodent fauna in the Erlian Basin, whereas cricetids and dipodids dominate in the Yuanqu Basin rodent fauna. The Ctenodactyloid *Gobiomys* is abundant and *Yuomys* is rare in the Erlian Basin, but *Yuomys*, *Xueshimys*, *Anadianomys* and *Zodiomys* are the common ctenodactyloids in the Yuanqu Basin. In addition to, the cylindrodontid rodent is present in the Erlian Basin but absent in the Yuanqu Basin. This difference may be related to the paleoclimate and paleoenvrionment of fossil area. On the basis of the compositions and characteristics of the plant fossils and pollen assemblages, Jin et al. (2003) divided the Eocene flora in China into three paleobotanical geographic regions, including a northern subtropical humid zone, a central subtropical arid zone and a southern tropical humid zone. The Erlian Basin belongs to the northern subtropical humid zone, in which the vegetation types are mainly deciduous trees

and shrubs interspersed with a few evergreens, and the vegetation diversity is high. The Yuanqu Basin is located in the central subtropical arid zone, where the vegetation is relatively scarce, and there are symbiotic angiosperms, gymnosperm, warm temperate and subtropical ferns, and a few subtropical and tropical evergreens. The different Sharamurunian rodent assemblages from the Erlian and Yuanqu basins probably indicate the different regional environments.

Table 11 Comparison of Sharamurunian rodent fossil assemblages from the Erlian Basin and the Yuanqu Basin

	Erlian Basin	Yuanqu Basin
cf. *Hulgana eoertnia*		√
Hulgana cf. *H. ertnia*	√	
cf. *Hulgana*. sp.		√
Protataromys mianchiensis		√
Yuomys cavioides	√	√
Yuomys magnus	√	
Xueshimys dissectus		√
Gobiomys neimongolensis	√	
Gobiomys asiaticus	√	
Gobiomys exiguus	√	
Anadianomys declivis		√
Zodiomys longmensis		√
Pappocricetodon rencunensis	√	√
Raricricetodon zhongtiaensis		√
Raricricetodon? *mino*		√
Primisminthus cf. *P. jinus*		√
Primisminthus shanghenus	√	√
cf. *Sinosminthus* sp.		√
Allosminthus uniconjugatus	√	√
Proardynomys ulausuensis	√	
Gobiocylindrodon sp.	√	

6 Conclusion

The new rodent materials discovered from the middle Eocene the lower part of the Shara Murun Formation of Ula Usu, Erlian Basin, Nei Mongol, China are identified as 9 species belonging to 7 genera, 4 families, and 1 superfamily of Rodentia. The new rodent assemblage has a high similarity with that of the “Lower Red” beds of the Erden Obo, and they jointly represent the Sharamurunian rodent fauna in the Erlian Basin. The analysis using the minimum number of individuals and the species richness shows that ctenodactyloids are the most abundant element comprising five species. In addition, dipodids represent 26.87% of the assemblage with *Allosminthus* being the dominant genus, but cricetids and ischyromyids are also present. Finally, with just two species present, cylindrodontids make up the smallest proportion of the rodent fauna in the Erlian Basin.

The Sharamurunian rodent fauna from the Erlian Basin is similar to the contemporaneous assemblage from the Yuanqu Basin, but there are distinct differences between these rodent faunas. The different compositions and characteristics of the Sharamurunian rodent faunas in

the Erlian and Yuanqu basins probably result from responses to the regional environmental disparity.

The Paleogene rodent assemblages of the Erlian Basin show a noticeable evolution from the dominance of ctenodactyloids in the Early Eocene to early Middle Eocene (Bumbanian to the Sharamurunian) to the dominance of cricetids and dipodids in the late Middle to Late Eocene (Ulangochuian and Ergilian).

Acknowledgements We thank Wang Yuanqing, Meng Jin, Bai Bin, Xu Rancheng, Wang Xiaoyang, Zhou Wei, Wang Yongxing, Wang Yongfu, Li Shijie, and Li Qi of the field team for their hard work and dedication. Hou Yemao and Yin Pengfei helped to perform the CT-scans. We also thank the editors and reviewers for their constructive comments on our manuscript. This work was supported by the National Natural Science Foundation of China (Grant no. 42072023) and the Strategic Priority Research Program of Chinese Academy of Sciences (XDB26000000, XDA20070203). The fieldwork was funded by the Special Fund for Fossil Excavation and Preparation, CAS.

中国内蒙古二连盆地沙拉木伦期啮齿类动物群研究

李 琪[1,2] 李 茜[2,3]

(1 云南大学生命科学学院脊椎动物演化研究中心 昆明 650500)

(2 中国科学院古脊椎动物与古人类研究所，中国科学院脊椎动物演化与人类起源重点实验室 北京 100044)

(3 中国科学院生物演化与环境卓越创新中心 北京 100044)

摘要：内蒙古二连盆地乌拉乌苏地区是亚洲哺乳动物分期中沙拉木伦期哺乳动物群的发现地和经典产地。在以往的研究中鲜少有关于这一地区啮齿类化石的研究。近来，在该地区沙拉木伦组下部地层中发现大量的啮齿类化石，经详细的形态学研究，它们被归入1超科4科7属9种，包括梳趾鼠超科的*Yuomys cavioides*, *Gobiomys neimongolensis*, *G. exiguus*以及*G. asiaticus*; 跳鼠科*Allosminthus uniconjugatus*和*Primisminthus shanghenus*; 仓鼠科*Pappocricetodon rencunensis*; 壮鼠科*Hulgana* cf. *H. ertnia*和圆柱齿鼠科*Proardynomys ulausuensis*。乌拉乌苏沙拉木伦组下部与额尔登敖包“下红层”的啮齿类组合具有高度相似性，两者共同构成了二连盆地沙拉木伦期啮齿类动物群。综合二连盆地乌拉乌苏地点沙拉木伦组下部以及额尔登敖包剖面“下红层”的啮齿类化石，运用最小个体数的方法对二连盆地沙拉木伦期啮齿类动物群的组分和特征进行了分析，结果显示梳趾鼠类最具优势，跳鼠类和仓鼠类次之。通过物种多样性分析，二连盆地古近纪啮齿类动物群呈现出早中始新世以梳趾鼠类为主导类群到晚始新世仓鼠、跳鼠类为主导类群的转变。内蒙古二连盆地和山西垣曲盆地沙拉木伦期啮齿类动物群的特征存在差异，很可能是由两个动物群所处不同的区域环境所造成的。

关键词：内蒙古，二连盆地，乌拉乌苏，沙拉木伦期，啮齿类动物群

References

Bai B, Wang Y Q, Li Q et al., 2018. Biostratigraphy and Diversity of Paleogene Perissodactyls from the Erlian Basin of Inner Mongolia, China. Am Mus Novit, 3914:1–60

Berkey C P, Granger W, 1923. Later sediments of the desert basins of central Mongolia. Am Mus Novit, 77: 1–16

Berkey C P, Morris F K, 1927. Geology of Mongolia—a reconnaissance report based on the investigations of the years 1922–1923. In: Natural History of Central Asia. Vol II. New York: American Museum of Natural History. 1–475

Burke J J, 1935. *Pseudocylindrodon*, a new rodent genus from the Pipestone Springs Oligocene of Montana. Ann Carnegie Mus, 25: 1–4

Burke J J, 1936. *Ardynomys* and *Desmatolagus* in the North American Oligocene. Ann Carnegie Mus, 25: 135–154

Chow M C, Rozhdestvensky A K, 1960. Exploration in Inner Mongolia – a preliminary account of the 1959 field work of the Sino-Soviet Paleontological Expedition (SSPE). Vert PalAsiat, 4: 1–10

Dashzeveg D, Meng J, 1998. A new Eocene cylindrodont rodent (Mammalia, Rodentia) from the eastern Gobi of Mongolia. Am Mus Novit, 3253: 1–18

Dawson M R, 1968. Oligocene rodents (Mammalia) from East Mesa, Inner Mongolia. Am Mus Novit, 2324: 1–12

Daxner-Höck G, 2001. New Zapodids (Rodentia) from Oligocene-Miocene deposits in Mongolia. Part 1. Senckenbergiana lethaea, 81: 351–389

Daxner-Höck G, Badamgarav D, Maridet O, 2014. Dipodidae (Rodentia, Mammalia) from the Oligocene and Early Miocene of Mongolia. Ann Naturh Mus Wien, Ser A, 116: 131–214

Douglass E, 1901. Fossil Mammalia of the White River Beds of Montana. Trans Am Philos Soc, Philadelphia, 20: 237–279

Emry R J, Tyutkova L A, Lucas S G et al., 1998. Rodents of the Middle Eocene Shinzhaly Fauna of eastern Kazakatan. J Vert Paleont, 18: 218–227

Fostowicz-Frelik Ł, Li C K, Meng J et al., 2012. New *Gobiolagus* (Mammalia: Lagomorpha) from the Middle Eocene of Erden Obo (Nei Mongol, China). Vert PalAsiat, 50: 219–236

Fostowicz-Frelik Ł, Li C K, Mao F Y et al., 2015. A large mimotonid from the Middle Eocene of China sheds light on the evolution of lagomorphs and their kin. Sci Rep, 9394: 1–9, doi: 10.1038/srep09394

Gong H, Li Q, Ni X J, 2021. New species of *Yuomys* (Rodentia, Ctenodactyloidea) from the upper Eocene of eastern Ningxia, China. J Vert Paleont, doi:10.1080/02724634.2021.1938099

Granger W, 1925. Records of fossils, Mongolia 1925. Third Central Asiatic Expeditions (Field Notes). New York: American Museum of Natural History. 1–76

Granger W, Berkey C P, 1922. Discovery of Cretaceous and older Tertiary strata in Mongolia. Am Mus Novit, 42: 1–7

Huang X S, Zhang J N, 1990. First record of Early Tertiary mammals from southern Yunnan. Vert PalAsiat, 28: 296–303

Jin J H, Liao W B, Wang B S et al., 2003. Global change in Cenozoic and evolution of flora in China. Guihaia, 23: 217–225

Li C K, 1975. *Yuomys*, a new ischyromyid rodent genus from the Upper Eocene of North China. Vert PalAsiat, 13: 58–70

Li C K, Ting S Y, 1983. The Paleogene mammals of China. Bull Carnegie Mus Nat Hist, 21: 1–93

Li Q, 2012. Middle Eocene Cricetids (Rodentia, Mammalia) from the Erlian Basin, Nei Mongol, China. Vert PalAsiat, 50: 360–364

Li Q, 2016. Eocene fossil rodent assemblages from the Erlian Basin (Inner Mongolia, China): Biochronological implications. Palaeoworld, 25: 95–103

Li Q, 2017. Eocene ctenodactyloid rodent assemblages and diversification from Erden Obo, Nei Mongol, China, Hist Biol, 31: 813–823

Li Q, 2018. Additional cricetid and dipodid rodent material from the Erden Obo section, Erlian Basin (Nei Mongol, China) and its biochronological implications. Palaeoworld, 27: 490–505

Li Q, 2020. New late Eocene cylindrodontid rodents from the Erlian Basin (Nei Mongol, China). Palaeobio Palaeoenv, 100: 1083–1094

Li Q, 2021. Additional tsaganomyid, cylindrodontid and ctenodactyloid rodent materials from the Erden Obo section, Erlian Basin (Nei Mongol, China). Vert PalAsiat, 59: 1–17

Li Q, Meng J, 2015. New ctenodactyloid rodents from the Erlian Basin, Nei Mongol, China, and the phylogenetic relationships of Eocene Asian ctenodactyloids. Am Mus Novit, 3828: 1–58

Li Q, Meng J, Wang Y Q, 2016. New cricetid rodents from strata near the Eocene–Oligocene boundary in Erden Obo Section (Nei Mongol, China). PloS One, 11: 1–17

Li Q, Gong Y X, Wang Y Q, 2017. New dipodid rodents from the Late Eocene of Erden Obo (Nei Mongol, China). Hist Biol, 29: 692–703

Li Q, Wang Y Q, Mao F Y et al., 2019. A new Eocene cylindrodontid rodent from the Erlian Basin (Nei Mongol, China) and its implications for phylogeny and biochronology. J Vert Paleont, 39: e1680990, doi: 10.1080/02724634.2019.1680990

Luterbacher H P, Ali J R, Brinkhuis H et al., 2004. The Paleogene Period. In: Gradstein F M, Ogg J G, Smith A eds. A Geological Time Scale 2004. Cambridge: Cambridge University Press. 384–408

Matthew W D, Granger W, 1925. New creodonts and rodents from the Ardyn Obo formation of Mongolia. Ibid, 197: 1–8

Matthew W D, Granger W, 1926. Two new perissodactyls from the Arshanto Eocene of Mongolia. Am Mus Novit, 208: 1–5

Meng J, Ye J, Huang X S, 1999. Eocene mammals from the Bayan Ulan of Nei Mongol (Inner Mongolia) and comments on related straigraphy. Vert PalAsiat, 37: 165–174

Romer A S, 1966. Vertebrate Paleontology. Chicago and London: University of Chicago Press. 1–467

Rose K D, 1981. The Clarkforkian land-mammal age and mammalian faunal composition across the Paleocene-Eocene boundary. Pap Palaeontol, 26: 1–197

Shi R L, 1989. Late Eocene mammalian fauna of Huangzhuang, Qufu, Shandong. Vert PalAsiat, 27: 87–102

Tong Y S, 1992. *Pappocricetodon*, a pre-Oligocene cricetid genus (Rodentia) from central China. Vert PalAsiat, 30: 1–16

Tong Y S, 1997. Middle Eocene small mammals from Liguanqiao Basin of Henan Province and Yuanqu Basin of Shanxi Province, Central China. Palaeon Sin, New Ser C, 26: 1–256

Tong Y S, Zheng S H, Qiu Z D, 1995. Cenozoic mammal ages of China. Vert PalAsiat, 33: 290–314

Speijer R P, Pälike H, Hollis C J et al., 2020. The Paleogene Period. In: Gradstein F M, Ogg J G, Schmitz M D et al. eds.

Geologic Time Scale 2020. Oxford: Elsevier BV. 1087–1140

Wang B Y, 1985. Zapodidae (Rodentia, Mammalia) form the Lower Oligocene of Qujing, Yunnan, China. Mainzer geowiss Mitt, 14: 354–367

Wang B Y, 1997a. The Mid-Tertiary Ctenodactylidae (Rodentia, Mammalia) of eastern and central Asia. Bull Am Mus Nat Hist, 234: 1–88

Wang B Y, 1997b. Chronological sequence and subdivision of Chinese Oligocene mammalian faunas. J Stratigr, 21: 183–191

Wang B Y, 2001. Eocene ctenodactyloids (Rodentia, Mammalia) from Nei Mongol, China. Vert PalAsiat, 39: 98–114

Wang B Y, 2007. Late Eocene cricetids (Rodentia, Mammalia) from Nei Mongol, China. Vert PalAsiat, 45: 195–212

Wang B Y, 2008. Additional rodent material from Houldjin Formation of Erenhot, Nei Mongol, China. Vert PalAsiat, 46: 2–30

Wang B Y, 2017. Discovery of *Yuomys* from Altun Shan, Xinjiang, China. Vert PalAsiat, 5: 227–232

Wang B Y, 2019a. “Cylindrodontidae”. In: Qiu Z X, Li C K eds. Palaeovertebrata Sinica, VIII, Basal Synapsids and Mammals, Fascicle 5, Glires II: Rodentia I. Beijing: Science Press. 449–478

Wang B Y, 2019b. “Gobiomyidae”. In: Qiu Z X, Li C K eds. Palaeovertebrata Sinica, VIII, Basal Synapsids and Mammals, Fascicle 5, Glires II: Rodentia I,. Beijing: Science Press. 436–440

Wang B Y, Dawson M R, 1994. A primitive cricetid (Mammalia: Rodentia) from the Middle Eocene of Jiangsu Province, China. Ann Carnegie Mus, 63: 239–256

Wang B Y, Zhou S Q, 1982. Late Eocene mammals from Pingchangguan Basin, Henan. Vert PalAsiat, 20: 203–215

Wang B Y, Wu W Y, Qiu Z D, 2020. “Cricetidae”. In: Qiu Z X, Li C K, Zheng S H et al. eds. Palaeovertebrata Sinica VIII, Basal Synapsids and Mammals, Fascicle 5, Glires II: Rodentia II. Beijing: Science Press. 10–151

Wang J W, 1978. Fossil Amynodontidae and Ischyromyidae of Tongbo, Henan. Vert PalAsiat, 16: 22–29

Wang Y Q, Meng J, Ni X J et al., 2007. Major events of Paleogene mammal radiation in China. Geol J, 42: 415–430

Wang Y Q, Meng J, Christopher K B et al., 2010. Early Paleogene stratigraphic sequences, mammalian evolution and its response to environmental changes in Erlian Basin, Inner Mongolia, China. Sci China Earth Sci, 53: 1918–1926

Wang Y Q, Meng J, Jin X, 2012. Comments on Paleogene localities and stratigraphy in the Erlian Basin, Nei Mongol, China. Vert PalAsiat, 50: 181–203

Wang Y Q, Li Q, Bai B et al., 2019. Paleogene integrative stratigraphy and timescale of China. Sci China Earth Sci, 62: 287–309

Wood A E, 1970. The Early Oligocene rodent *Ardynomys* (Family Cylindrodontidae) from Mongolia and Montana. Am Mus Novit, 2418: 1–18

Woodburne J M, 1987. Mammal ages, stages, and zones. In: Woodburne M O ed. Cenozoic Mammals of North America: Geochronology and Biostratigraphy. Berkeley: University of California Press. 18–23

Vandenberghe N, Hilgen F L, Speijer R P, 2012. The Paleogene Period. In: Gradstein F M, Ogg J G, Schmitz M D et al. eds. The Geologic Time Scale 2012. Oxford: Elsevier BV. 855–922

Ye J, 1983. Mammalian fauna from the Late Eocene of Ulan Shiren Area, Inner Mongolia. Vert PalAsiat, 21: 109–118

Zdansky O, 1930. Die alttertiären Säugetiere Chinas nebst stratigraphischen Bemerkungen. Palaeont Sin, New Ser C, 6: 1–87